

Temperature-dependent evolution of grain growth in mullite fibres

Martin Schmücker^{a,*}, Hartmut Schneider^a, Thomas Mauer^b, Bernd Clauß^b

^a German Aerospace Center (DLR), Institute of Materials Research, Germany

^b Institute for Textile Chemistry and Chemical Fibres, Koerschstalstr. 26, D-73770 Denkendorf, Germany

Received 30 April 2004; received in revised form 5 August 2004; accepted 15 August 2004

Abstract

Mullite grain size characteristics of four different alumino silicate fibres heat-treated between 1400 and 1700 °C in a time frame of 0.5–100 h have been determined. Mullite grain sizes show little change up to 1500 °C though the grain microstructure develops from mosaic-type to faceted. Above 1500 °C grain growth kinetics follow the empirical law $D^{1/n} - D_0^{1/n} = kt$ (D_0 = initial grain size, D = grain size after annealing, $1/n$ = grain growth exponent, k = reaction constant, and t = firing time). Between 1500 and 1600 °C the grain growth exponent is remarkably low ($1/n = 1/12$) but above 1600 °C grain growth exponents reach normal values of $\approx 1/3$. The vacancy drag model has been used to explain the complex grain growth behaviour of mullite.

© 2004 Elsevier Ltd. All rights reserved.

Keywords: Grain size; Fibres; Mullite; Electron microscopy; Grain growth

1. Introduction

Due to its outstanding properties including high thermal and chemical stability, low thermal expansion,¹ low thermal conductivity² and high creep resistance³ mullite ($\approx 3\text{Al}_2\text{O}_3 \cdot 2\text{SiO}_2$) is a strong candidate material for structural applications under thermal and mechanical load. Although mullite is one of the most widely studied ceramic materials no comprehensive quantitative work has been published on its temperature-induced grain growth. This is in spite of the well-known fact that even small grain coarsening has a strong negative influence on the mechanical behaviour, especially in case of ceramic fibres.^{4–6} Densification and grain growth kinetics of mullite ceramics were first investigated by Ghate et al.⁷ Both effects were assumed to be controlled by the diffusion of Si^{4+} . Later on, Huang et al.⁸ investigating the microstructures of hot-pressed mullite ceramics (“stoichiometric” composition, i.e. 72 wt.% Al_2O_3 , 28 wt.% SiO_2) found that the grain size evolution of mullite is slow below 1590 °C and that the mullite grains remain virtually equiax-

ial. Above 1590 °C, strong and acicular grain growth occurs, which has been explained by enhanced diffusion in the presence of a liquid silicate phase that forms in case of silica-rich mullite (Fig. 1). A quantitative study on the mullite grain growth of a laboratory-produced (75 wt.% Al_2O_3 , 25 wt.% SiO_2) and of a commercial alumino silicate fibre (Nextel 720; 85 wt.% Al_2O_3 , 15 wt.% SiO_2) has been published by Schmücker et al.⁹ recently. The fibres were overstoichiometric with respect to the Al_2O_3 content and hence were less prone to the formation of a coexisting silicate melt (Fig. 1). Due to the high Al_2O_3 contents the fibres contain different amounts of α -alumina besides the main phase mullite. Schmücker et al. showed, that isothermal mullite grain growth follows the empirical law:

$$D^{1/n} - D_0^{1/n} = kt \quad (1)$$

with D_0 = initial grain size, D = grain size after annealing, $1/n$ = grain growth exponent, k = reaction constant, and t = firing time (e.g. ref. 10).

Two temperature regimes with respect to the observed grain growth exponents have been distinguished: Below 1600 °C the grain growth exponent is remarkably small ($1/n \approx 1/12$), while above 1600 °C grain growth exponents

* Corresponding author. Tel.: +49 2203 6012462; fax: +49 2203 696480.
E-mail address: martin.schmuecker@dlr.de (M. Schmücker).

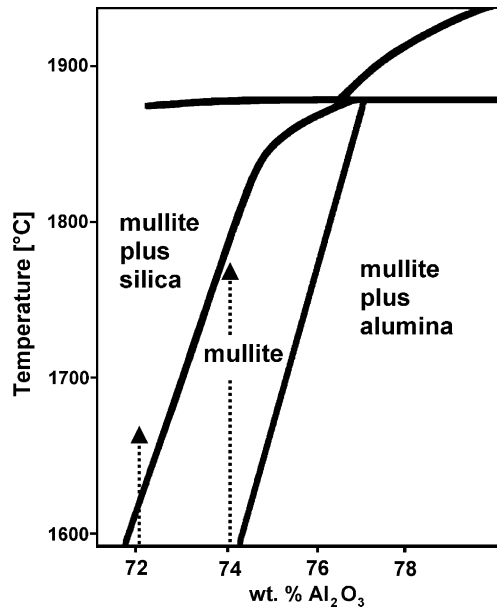


Fig. 1. Mullite region of the Al_2O_3 - SiO_2 phase diagram (after Klug et al.²¹).

reach typical values of $\approx 1/3$. The fibre composition and the uniform grain size distribution occurring in both temperature regimes militates against the idea that the changing grain growth behaviour is caused by the formation of a siliceous melt but should have other reasons. It is the aim of this study to provide more experimental grain growth data and to further contribute to the understanding of the grain growth mechanisms.

2. Experimental

2.1. Fibre material

To analyze grain growth kinetics of mullite, alumino silicate fibres with a composition of 64 mol% Al_2O_3 , 36 mol% SiO_2 (75 wt.% Al_2O_3 , 25 wt.% SiO_2) were prepared: Mu-1 contains ≈ 200 ppm Na as major impurity, while Mu-2 is an ultra-high purity mullite fibre (Na-content below 1 ppm). For reasons of comparison, commercial Nextel (3M) fibres 550 and 720 were investigated, additionally (Table 1).

Table 1
Fibre samples used for the temperature-induced grain growth analysis

Fibre type	Manufacturer	Composition	Phase content	Reference
Nextel 550	3M	73 wt.% Al_2O_3 , 27 wt.% SiO_2	Transition alumina plus SiO_2 after firing at 1350 °C, 1h: mullite	11
Nextel 720	3M	85 wt.% Al_2O_3 , 15 wt.% SiO_2	Mullite plus α -alumina	12
Mu-1	This work	75 wt.% Al_2O_3 , 25 wt.% SiO_2 , ≈ 200 ppm Na (impurity)	Mullite plus traces of α -alumina	
Mu-2	This work	75 wt.% Al_2O_3 , 25 wt.% SiO_2 , <1 ppm Na	Mullite plus traces of α -alumina	

2.1.1. Laboratory-produced fibres Mu-1, Mu-2

The production of mullite ceramic fibres on the lab scale was conducted by dry-spinning of a mullite forming spinning solution with adequate rheology, and subsequent pyrolysis and sintering of the green fibres. The process yields ceramic fibres with diameters between 10 and 12 μm . The spinning solution was prepared by using basic aluminum chloride $\text{Al}_2(\text{OH})_5\text{Cl}\cdot(2-3)\text{H}_2\text{O}$, aqueous 20 nm SiO_2 -sol, polyvinylpyrrolidone (PVP) and water. The components are first mixed in the proper stoichiometry (64 mol% Al_2O_3 , 36 mol% SiO_2) leading to an oxide yield of about 30 wt.%. The aqueous solution is then concentrated to a viscoelastic solution with good spinning properties. Typically zero shear viscosities of the solutions at 25 °C range between 200 and 400 Pa. The spinning solution is spun by a dry spinning process with a 90 hole spinneret having hole diameters of 100 μm . At winding speeds between 150 and 200 m/min a green fibre multifilament with fibre diameters of 15–17 μm are obtained. A technique was developed to cross-wind the green fibres on a bobbin and store them until they are further processed to ceramic fibres.

Green fibres are pyrolyzed and sintered to ceramic fibres with a heating rate of 3 K/min up to 1100 °C during pyrolysis and 15 K/min to the end temperature of 1300 °C. The fibres are then cooled down to room temperature without controlled cooling rate. Chemical compositions and the phase contents of the laboratory-produced fibres Mu-1 and Mu-2 are summarized in Table 1.

2.1.2. Commercial fibres (Nextel 550, Nextel 720)

Nextel 550 alumino silicate fibres consist of transition alumina plus vitreous silica with a bulk composition of 73 wt.% Al_2O_3 , 27 wt.% SiO_2 .¹¹ The starting assemblage transforms to single phase mullite of $\approx 0.4 \mu\text{m}$ grain sizes after firing at 1300 °C. The composition of Nextel 720 fibres is 85 wt.% Al_2O_3 , 15 wt.% SiO_2 . These fibres consist of mosaic-type mullite crystals of 0.3–0.5 μm in diameter which enclose α -alumina grains of 50–100 nm.¹² All Nextel fibres investigated stem from 3M (St. Paul, MN, USA) and are fabricated by sol-gel techniques.^{6,13}

2.1.3. Heat treatments of the fibres

Heat treatments of the fibres were carried out in a laboratory furnace between 1400 and 1700 °C with dwell times between 0.5 and 100 h.

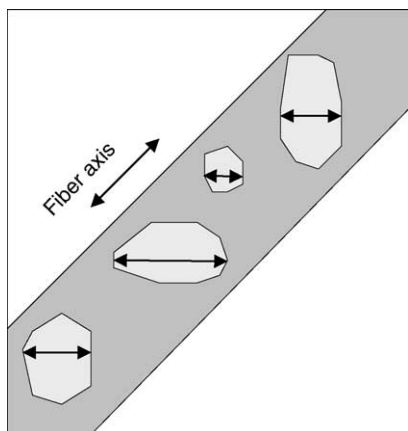


Fig. 2. Sketch illustrating the strategy of grain size determination.

2.2. Grain size analysis

The grain size analyses of the heat-treated fibres were carried out by means of a LEO Gemini DSM 982 scanning electron microscope (SEM) equipped with a field emission gun. After embedding in phenolic mounting resin fibre length sections were prepared by grinding and polishing and subsequent chemical etching. The chemical etchant consisted of an admixture of HF, H₂O₂ and HNO₃ in a ratio of 6:5:1. The average grain size was determined by gaging all well-defined grains of the respective micrographs. Grain size was defined as maximum extension in horizontal direction (see Fig. 2). To avoid mismeasurements in case of possible textured grain distributions, all micrographs were taken in a way that the fibre axis corresponds to the image diagonal.¹⁴ The grain size determination included at least 250 grains per analyzed sample. Measurements of length were performed using the image analysis software “Scion image” (Scion Corp. Frederick, MD, USA). Additional to SEM analyses, the starting fibres were investigated by transmission electron microscopy (TEM) using a Philips Tecnai F30 microscope equipped with a STEM unit.

3. Results and discussion

The microstructure of the laboratory-produced mullite fibre Mu-1 after firing at 1300 °C (1 h) is shown in Fig. 3. The fibres consist of mullite with mosaic-type grains of up to 500 nm in diameter, having wavy contours and some intragranular porosity (see also Fig. 5). The mosaic-type morphology is typical for mullites crystallized from diphasic precursors.¹ Sporadically, small alumina inclusions appear within the mullite grains. The microstructures of the laboratory-scale fibre Mu-2 and of the commercial fibre Nextel 550 heat-treated in the same way as Mu-1 are very similar.

¹ Diphasic mullite precursors typically consist of transition alumina plus vitreous silica.

The commercial Nextel 720 fibre, on the other hand, displays numerous small alumina grains (mean diameter: ≈ 80 nm) occurring within the mosaic-type mullite crystals (Fig. 4). Fig. 5 shows the microstructural evolution of Mu-1 fibres after firing for 1 h between 1300 and 1700 °C. Below ≈ 1550 °C only little grain growth occurs even after long-term heat-treatments, but gradually the grain morphologies change from irregular shaped to faceted and the intragranular porosity disappears. Heat-treatments of 1600 °C and above, however, produce a much higher time dependency of grain growth (Fig. 6). This finding is illustrated in Fig. 7 showing as an example the microstructure of Mu-1 fibres after heat-treatments of 1, 8, and 32 h at 1500 and 1600 °C, respectively. The ultra-pure laboratory-scale fibre Mu-2, and the commercial Nextel 550 and 720 alumino silicate fibres display a similar behaviour with the time dependency of grain coarsening being very small below 1600 °C but rather high above 1600 °C. In case of the Nextel 550 fibres (Table 1) the high temperature behaviour could not be analyzed unambiguously, due to secondary grain growth. This probably is caused by the presence of a liquid silicate phase forming above ≈ 1600 °C due to the relatively high SiO₂ content of this fibre (see Huang et al.⁸ and Fig. 1). Kinetic data are summarized in Fig. 8 in a $\ln D$ versus $\ln t$ plot (D = grain diameter, t = dwell time). Grain growth curves are straight lines with slopes corresponding to the grain growth exponent $1/n$ in a first approximation. The determination of the grain growth exponents, however, was performed by fitting the experimental data to Eq. (1) using D_0 -values of 355 nm (Mu-1), 280 nm (Mu-2), 400 nm (Nextel 550) and 320 nm (Nextel 720). As shown in Fig. 9 average grain growth exponents are about 1/12 and 1/3 for temperatures below and above 1600 °C, respectively. On the basis of the average grain growth exponents reaction constants $k(T)$ have been calculated for Mu-1, Nextel 550 and Nextel 720 and are plotted in an Arrhenius diagram (Fig. 10). The effective activation energy of grain growth is ≈ 900 kJ/mol for all fibres below and above 1600 °C. This value is higher than those published on the basis of sintering data (≈ 700 kJ/mol)^{3,7,15} but corresponds to the activation energy of mullite creep.^{16,17}

While grain growth exponents above 1600 °C ($1/n \approx 1/3$) are in the range of growth exponents typically found in ceramics (e.g. Kingery et al.¹⁸), the growth exponents below 1600 °C are extremely small ($1/n \approx 1/12$). Similar low values have been described for nanocrystalline metals¹⁰ with the same tendency, i.e. showing increasing exponents with increasing firing temperature. In general, deviations of the grain growth exponents from the theoretical value near $n = 1/2$ are attributed to reduced grain boundary mobility, caused by grain boundary segregations, solute drag, second phase drag or due to the fact that the sample size inhibits grain growth.^{10,18} The latter is excluded because the fibre diameters are well above the mullite grain sizes. Moreover, careful transmission electron microscopic investigations did not provide any evidence for impurity segregations or second phase agglomerations at the grain boundaries of mullite. It can-

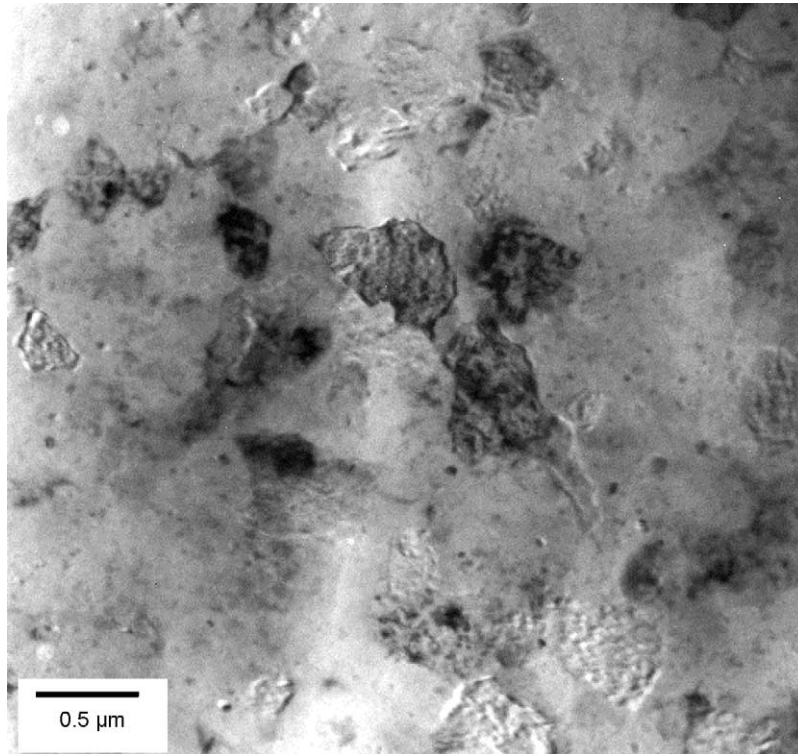


Fig. 3. Starting state of the laboratory-produced mullite fibre Mu-1 (transmission electron micrograph). The fibre consists of irregular shaped mosaic-type mullite crystals.

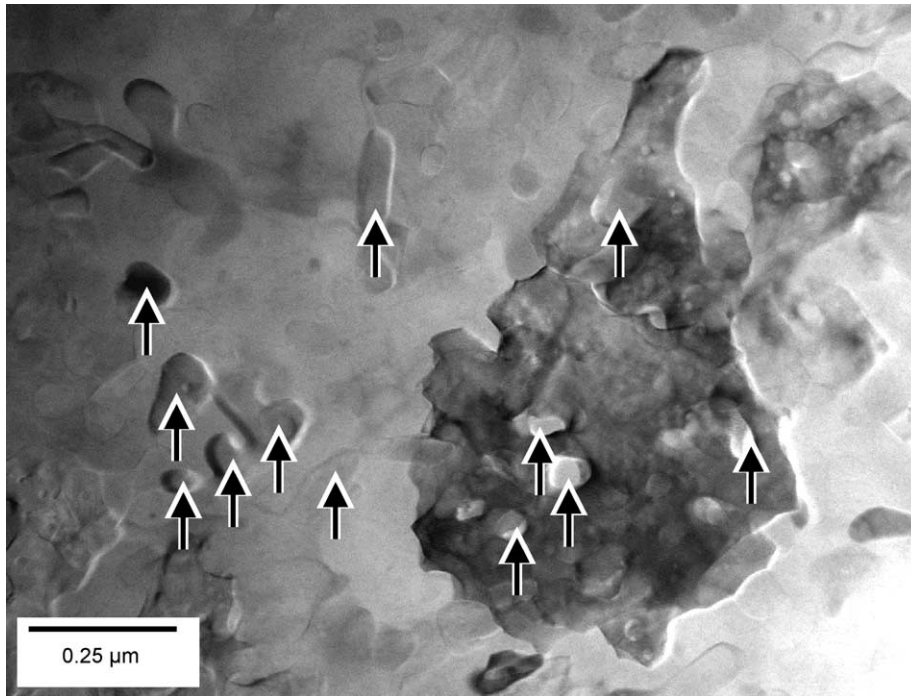


Fig. 4. Starting state of commercial Nextel 720 fibres (transmission electron micrograph). Small alumina grains (≈ 80 nm) are embedded in the mosaic-type mullite grains.

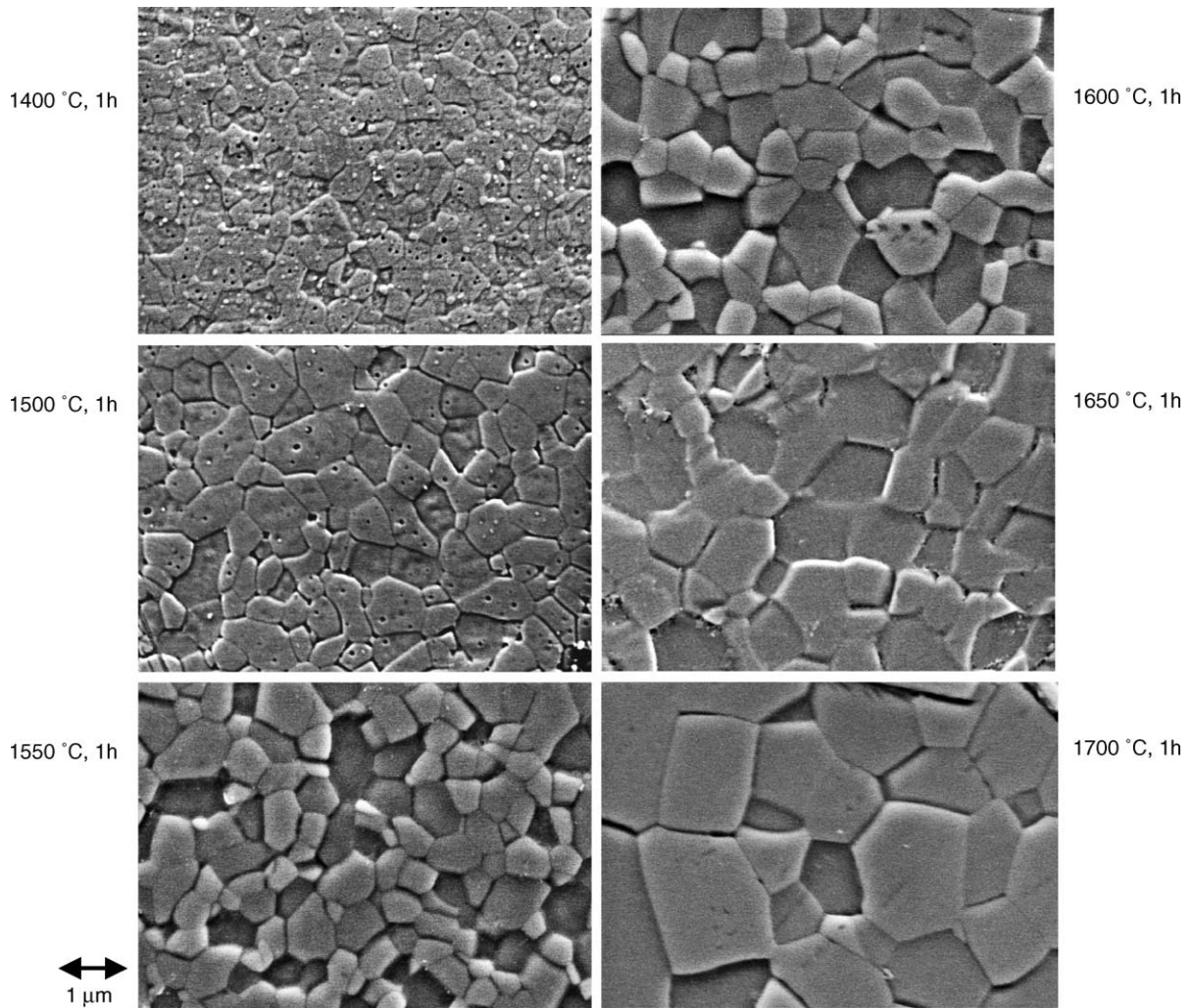


Fig. 5. Microstructural evolution of Mu-1 fibres after firing for 1 h between 1300 and 1700 °C.

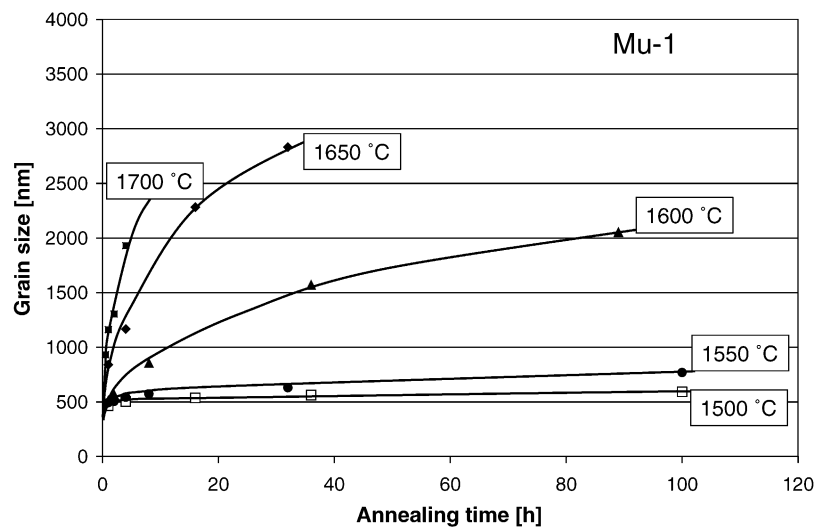


Fig. 6. Grain size evolution of Mu-1 fibres due to isothermal heat-treatments between 1500 and 1700 °C.

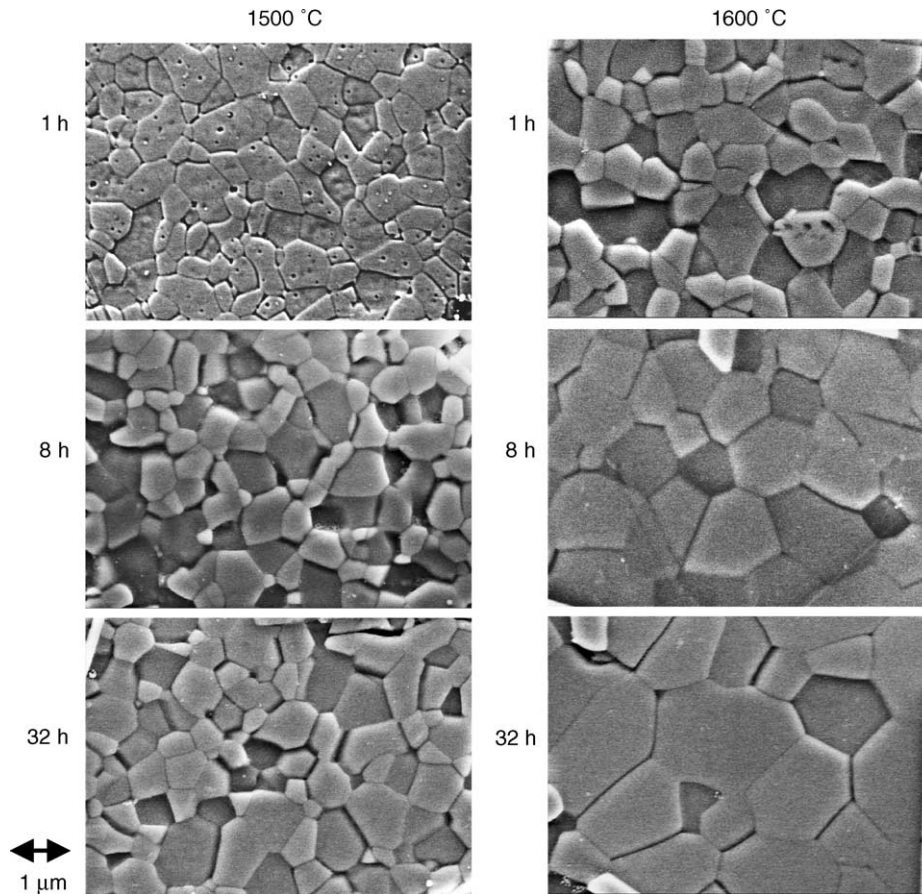


Fig. 7. Microstructural evolution of Mu-1 fibres due to isothermal heat-treatments at 1550 and 1600 °C. Time dependency of grain growth changes significantly between 1550 and 1600 °C.

not be ruled out that traces of impurities do affect the low temperature grain growth behaviour, but the fact that mullite fibres with clearly different amounts of impurities display virtually the same grain growth kinetics accounts against this idea.

A novel explanation of the retarded low-temperature grain growth behaviour may be derived from specifics of the mullite crystal structure together with the “vacancy drag” model (e.g. Estrin¹⁹). The idea behind this concept is that grain growth corresponds to a gradual decrease of grain bound-

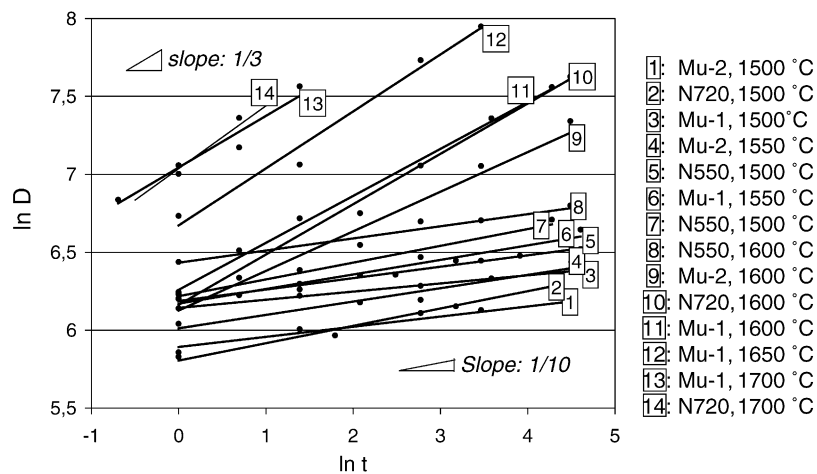


Fig. 8. Grain size vs. dwell time in logarithmic presentation. Estimated grain growth exponents are about 1/10 if the firing temperature is below 1600 °C (lines 1–8) but change to about 1/3 at higher temperatures (lines 9–14).

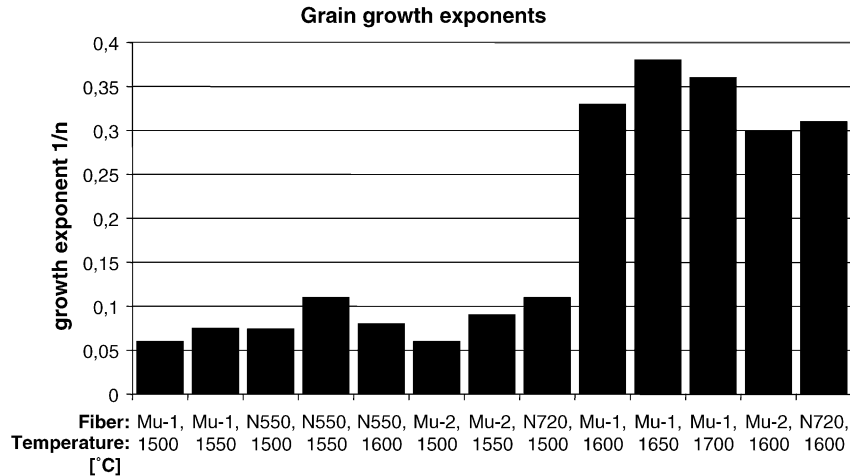


Fig. 9. Grain growth exponents of Mu-1, Mu-2, Nextel 550, and Nextel 720 fibres fired between 1500 °C and 1700 °C. Data are obtained by fitting the experimental value to Eq. (1).

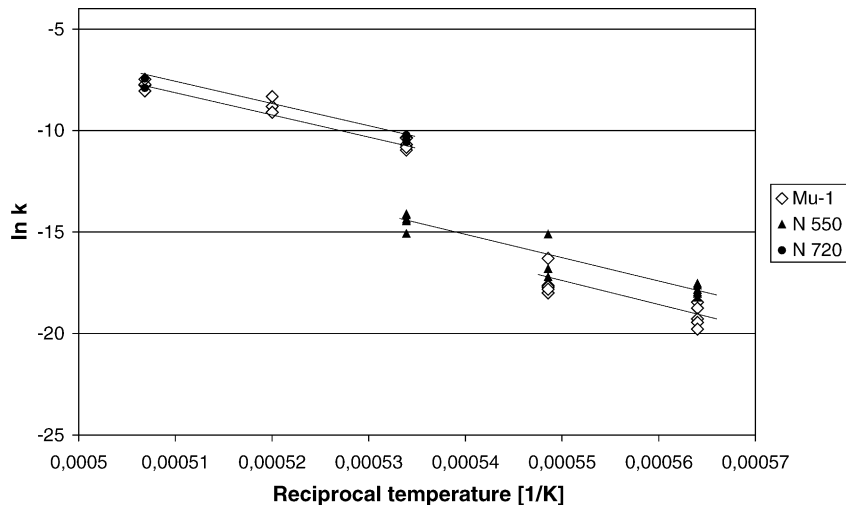


Fig. 10. Reaction constants of grain growth vs. temperature in Arrhenius presentation. The reaction constants k are calculated on the basis of average grain growth exponents of 1/12 (“low”-temperature regime), or 1/3 (“high”-temperature regime), respectively.

ary phase accompanied with release of excess free volume via vacancies. According to this model the grain growth rate is controlled by the diffusion of vacancies through the bulk. Though vacancy drag is considered to be a general effect, there is some evidence that it may have special importance for mullite. Actually, vacancies play a particular role in the structure of mullite as excess positive charges arising by increasing Al/Si ratios are compensated by “structural” oxygen vacancies at specific crystallographic sites.²⁰ Thus, it could be envisaged that additional oxygen vacancies arising by a reduction of grain boundaries are related to changes in local composition. As a consequence, the diffusion of excess vacancies towards a vacancy sink may go along with local compositional fluctuations of the respective mullite crystal. Due to the coupling of vacancy concentration with the local composition, vacancy diffusion in mullite is considered to be sluggish, thus leading to sluggish grain growth. Above

the threshold temperature of ≈ 1600 °C, however, the equilibrium composition of mullite becomes richer in alumina (see Fig. 1). For reasons of charge compensation the concentration of structural oxygen vacancies has to increase. Thus, excess vacancies generated by the decrease of grain boundaries may be trapped as structural vacancies in the mullite structure, and hence the necessity of long-range vacancy migration toward external sinks is reduced.

Acknowledgements

The authors wish to thank Deutsche Forschungsgemeinschaft (DFG) for financial support. Mr. K. Baumann assisted in ceramographic sample preparation which is greatly appreciated. Basic aluminum chloride was provided by Clariant (Gersthofen, Germany) which is gratefully acknowledged.

References

1. Schneider, H. and Eberhard, E., Thermal expansion of mullite. *J. Am. Ceram. Soc.*, 1990, **73**, 2073–2076.
2. Schneider, H., Okada, K. and Pask, J. A., *Mullite and Mullite Ceramics*. John Wiley & Sons, Chichester, 1994.
3. Dokko, P. C., Pask, J. A. and Mazdiyasi, K. S., High temperature mechanical properties of mullite under compression. *J. Am. Ceram. Soc.*, 1977, **60**, 150–155.
4. Schmücker, M., Flucht, F. and Schneider, H., High-temperature behaviour of polycrystalline alumo-silicate fibres with mullite bulk composition. I. Microstructure and strength properties. *J. Eur. Ceram. Soc.*, 1996, **16**, 281–286.
5. Schneider, H., Göring, J., Schmücker, M. and Flucht, F., Thermal stability of Nextel 720 alumino silicate fibres. In *Ceramic Microstructures*, ed. A. P. Tomsia and A. M. Glaeser. Plenum Press, New York, 1998, pp. 721–728.
6. Deléglise, F., Berger, M. H. and Bunsell, A. R., Microstructural evolution under load and high temperature deformation mechanisms of a mullite/alumina fibre. *J. Eur. Ceram. Soc.*, 2002, **22**, 1501–1502.
7. Ghate, B. B., Hasselmann, D. P. H. and Spriggs, R. M., Kinetics of pressure sintering and grain growth of ultra-fine mullite powder. *Ceram. Int.*, 1975, **1**, 105–110.
8. Huang, T., Rahaman, M. N., Mah, T. and Parthasarathy, T. A., Anisotropic grain growth and microstructural evolution of dense mullite above 1550 °C. *J. Am. Ceram. Soc.*, 2000, **83**, 204–210.
9. Schmücker, M., Schneider, H., Mauer, T. and Clauß, B., Kinetics of mullite grain growth in alumino silicate fibres. *J. Am. Ceram. Soc.*, in press.
10. Malow, T. R. and Koch, C. C., Grain growth in nanocrystalline iron prepared by mechanical attrition. *Acta Mater.*, 1997, **45**, 2177–2186.
11. *3M Ceramic Textile and Composite: Nextel™ Technical Notebook*.
12. Wilson, D. M., Lieder, S. L. and Lueneburg, D. C., Microstructure and high temperature properties of Nextel 720 fibres. *Ceram. Eng. Sci. Proc.*, 1995, **16**, 1005–1014.
13. Chawla, K. K., *Ceramic Matrix Composites*. Kluwer, Boston, 2003.
14. Schmücker, M., Flucht, F. and Schneider, H., Temperature stability of 3M Nextel 610, 650, and 720 fibres—a microstructural study. In *High Temperature Ceramic Matrix Composites*, ed. W. Krenkel, R. Naslain and H. Schneider. Wiley, VCH, Weinheim, 2001, pp. 74–78.
15. Sacks, M. D. and Pask, J. A., Sintering of mullite containing materials. *J. Am. Ceram. Soc.*, 1982, **65**, 65–70.
16. Kumazawa, T., Kanzaki, S., Wakai, T. and Tabate, H., Creep of mullite ceramics. In *Proceedings of the 25th Symposium on the Basic Science of Ceramics*, Paper No. 1E08. Ceramic Society of Japan, Tokyo, 1987.
17. Ohira, H., Shiga, H., Ismail, M. G., Nakai, Z., Akiba, T. and Yasuda, E., Compressive creep of mullite ceramics. *J. Mater. Sci. Lett.*, 1991, **10**, 847–849.
18. Kingery, W. D., Bowen, H. K. and Uhlmann, D. R., *Introduction to Ceramics (2nd ed.)*. John Wiley & sons, New York, 1976, pp. 454–460.
19. Estrin, Y., Vacancy effects in grain growth. In *Proceedings of the First Joint International Conference “Recrystallization and Grain Growth”*, ed. G. Gottstein and D. A. Molodov. Springer, Heidelberg, 2001, pp. 135–140.
20. Angel, R. J. and Prewitt, C. T., Crystal structure of mullite: a re-examination of the average structure. *Am. Min.*, 1986, **71**, 1476–1482.
21. Klug, F. J., Prochazka, S. and Doremus, R. H., Alumina-silica phase diagram in the mullite region. *J. Am. Ceram. Soc.*, 1987, **70**, 750–759.